Charge-recombination processes in oligomer- and polymer-based light-emitting diodes: A molecular picture

David Beljonne
Zhigang Shuai
AiJun Ye
Jean-Luc Brédas

Abstract — An overview of our recent work on the mechanisms of singlet and triplet exciton formation in electroluminescent π-conjugated materials will be presented. According to simple spin statistics, only one-fourth of the excitons are formed as singlets. However, deviations from that statistics can occur if the initially formed triplet charge-transfer (CT) excited states are amenable to intersystem crossing or dissociation. Although the electronic couplings between the CT states and the neutral exciton states are expected to be largest for the lowest singlet and triplet excitons (S_1 and T_1, respectively), the possibility for direct recombination into T_1 is always very small due to the large exchange energy. In small molecules, spin statistics is expected to be observed because both singlet and triplet exciton formations proceed *via* higher-lying S_n/T_n states with similar electronic couplings and fast formation rates. In extended conjugated chains, however, that the $^1CT \rightarrow S_1$ pathway is faster while the $^3CT \rightarrow T_n$ channels become much slower, opening the route to intersystem crossing or dissociation among the ^3CT states.

Keywords — *Organic light-emitting diodes, polymer light-emitting diodes, singlet and triplet excitons, charge transfer, charge recombination, intersystem crossing.*

1 Introduction

Recently, the electronics and photonics technologies have opened their materials base to organics, in particular π-conjugated oligomers and polymers. The goal with organics-based devices is not necessarily to attain or exceed the level of performance of inorganic semiconductor technologies (silicon is still the best at many things it does) but to benefit from a unique set of characteristics combining the electrical properties of (semi)conductors with the properties typical of plastics, *i.e.*, low cost, versatility of chemical synthesis, ease of processing, and flexibility. Interest in conjugated polymers picked up significantly after the 1976 discovery that they can be made highly electrically conducting following a redox chemical treatment.[1] This discovery led to the 2000 Nobel Prize in Chemistry awarded to Alan Heeger, Alan MacDiarmid, and Hideki Shirakawa. By the mid-eighties, many research teams both in academia and industry were investigating π-conjugated oligomers and polymers for their nonlinear optical properties or their semiconducting properties, paving the way to the emergence of the fields of plastic electronics and photonics.[2]

The technological developments in plastic electronics and photonics have required researchers to gain a much better fundamental understanding of the nature of electronic excitations, charge carriers, and transport phenomena in ordered and disordered π-conjugated materials. Our aim in this contribution is to review some issues related to charge recombination in oligomer- and polymer-based light-emitting diodes, which will highlight the fascinating chemistry and physics of these materials and the strong connection there exists in this field between basic and applied research.

A major breakthrough in the field of organic electronics is the 1987 report by Tang and Van Slyke at Kodak of the first electroluminescent device based on a π-conjugated molecular material, tris(8-hydroxy-quinoline) aluminum (Alq_3).[3] Shortly thereafter, Friend and his group at Cambridge discovered electroluminescence in a conjugated polymer, poly(para-phenylenevinylene), thereby opening the way for the fabrication of polymer light-emitting diodes (LEDs).[4]

Typically, an organic LED is built[5] by depositing successively on a transparent substrate: a transparent electrode made of a high-work-function metal, usually indium tin oxide (ITO); one or several organic layers that in the case of molecular materials are generally deposited by vacuum sublimation[6] or in the case of polymers by spin-coating or ink-jet printing[7]; and a top metallic electrode made of a low-work-function metal or alloy. Four main steps are required to generate light from a LED device upon application of a forward bias:

(i) **Charge injection:** electrons (holes) are injected from the Fermi level of the low- (high) work-function metal into the lowest unoccupied (highest occupied) electronic levels of the organic material present at the metal-organic interface;

Received 01/01/05; accepted 01/26/05.

D. Beljonne is with the University of Mons-Hainaut, Laboratory for Chemistry of Novel Materials, Belgium, and the School of Chemistry and Biochemistry, Georgia Institute of Technology, Atlanta, GA, U.S.A.

Z. Shuai is with the Center for Molecular Science, Institute of Chemistry, The Chinese Academy of Sciences, Beijing, P. R. China.

A. Ye is with the School of Chemistry and Biochemistry, Georgia Institute of Technology, Atlanta, GA, U.S.A.

J-L. Brédas is with the School of Chemistry and Biochemistry, Georgia Institute of Technology, Atlanta, GA, U.S.A. and the University of Mons-Hainaut, Laboratory for Chemistry of Novel Materials, Belgium; telephone 404/385-4986, e-mail: jean-luc.bredas@chemistry.gatech.edu.

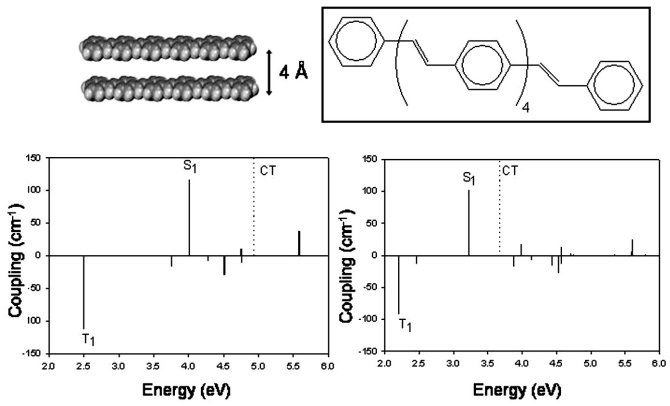

FIGURE 1 — Top: Illustration of the cofacial configuration between two OPV6 oligomers (left); chemical structure of OPV6 (right). Bottom: Charge recombination electronic couplings, V_{if}, into singlet and triplet excited states in cofacial dimers of OPV2 (left) and OPV6 (right) molecules. For the sake of clarity, V_{if} values are reported as positive and negative values for singlets and triplets, respectively. The PPP/SCI excitation energies from the singlet ground state to the lowest singlet and triplet excited states are shown on the abscissa axis. The approximate energetic position of the lowest charge-separated state, as obtained from AM1/CI/COSMO calculations, is indicated by the dashed line. The molecular packing is shown on top.

(ii) **Charge transport:** electrons and holes drift in opposite directions within the organic layer(s) (usually in a dispersive manner) under the influence of the static electric field generated by the forward bias;

(iii) **Charge recombination:** electrons and holes approaching one another can capture and recombine to lead to the formation of either singlet or triplet excitons; during their lifetime, excitons can hop among molecules/chains *via* energy-transfer processes;

(iv) **Excitation decay:** when excitons decay radiatively, the generated light can escape from the device through the transparent side.

In electrophosphorescent diodes, a phosphorescent dye is present as guest in a host matrix and exciton transfer can take place from the host matrix to the guest; high efficiencies are reached since both singlet and triplet excitations generated in the host can transfer to the guest and contribute to the luminescence signal. In conjugated polymer LEDs, in the absence of phosphorescent dyes, only singlet excitons generate light.

Organic light-emitting diodes have recently entered the market place as active elements in low-resolution displays such as those commercialized, for instance, by Pioneer in car stereo systems, by Kodak in digital cameras, or by Philips in electric shavers. The production of high-resolution full-color flexible displays for television screens is the next target.

This brief description highlights the importance of electron-transfer and energy-transfer processes into or within the π-conjugated materials. Thus, the design of new materials with optimal performance requires a fundamental understanding of these processes, which we briefly describe in Section 2. However, our main goal in this contribution is to review, in Section 3, some of our recent work that addresses *at the molecular level* the nature of the main parameters that govern electron-recombination processes in oligomer- and polymer-based light-emitting diodes. Our emphasis is on the rates of formation of the lowest singlet and triplet excited states in *p*-phenylenevinylene chains and their evolutions with chain length. The chemical structure of *p*-phenylenevinylene chains is shown on top of Fig. 1.

2 Electron- and energy-transfer processes

It is useful to point out that both electron-transfer and energy-transfer processes are driven by similar electron-electron and electron-vibration interactions. As a result, they can be described by similar mathematical formalisms, a fact especially clear in the case of weak electronic interactions. Both processes can be viewed as special cases of the non-radiative decay of an electronic state. In the framework of perturbation theory,[8–10] the probability for a transition from a discrete initial state ψ_i (corresponding to the reactants) to a discrete final state ψ_f (corresponding to the products of the reaction) writes under application of a perturbation V to first order:

$$P_{if} = \frac{1}{\hbar^2}\left|\left\langle \psi_i|V|\psi_f \right\rangle\right|^2\left(\frac{\sin(\omega_{fi}t/2)}{\omega_{fi}/2}\right), \qquad (1)$$

where t denotes time, ω_{fi} the transition energy between the electronic states i and f, and $\langle\psi_i|V|\psi_f\rangle$ is the corresponding electronic-coupling matrix element. To account for a continuous distribution of final (vibrationally coupled) electronic states, Eq. (1) can be recast by introducing the density of final states, $\rho(E_f)$, and summing over all probability densities. Assuming that the function $|\langle\psi_i|V|\psi_f\rangle|^2\rho(E_f)$ varies smoothly with energy, the transition probability per unit time (or transition rate) adopts, in the long-time limit, the simple and widely exploited Fermi's Golden Rule form:

$$k_{if} = \frac{2\pi}{\hbar}\left|\left\langle \psi_i|V|\psi_f \right\rangle\right|^2\rho(E_f). \qquad (2)$$

In both electron- and energy-transfer cases, the transition mechanism involves vibrational motions driving the reaction coordinates from reactants to products. The expression for the rate obtained within the Frank–Condon approximation factorizes into an electronic and a vibrational contribution as:

$$k_{if} = \frac{2\pi}{\hbar}\left|V_{if}\right|^2(FCWD). \qquad (3)$$

Here, $V_{if} = \langle\psi_i|V|\psi_f\rangle$ is the electronic-coupling matrix element and (FCWD) denotes the Franck–Condon-weighted density of states. In the high-temperature regime, *i.e.*, when

assuming that all vibrational modes are classical ($\omega_i << k_\Omega T$), the FCWD obeys a standard Arrhenius-type equation:

$$(FCWD) = \frac{1}{\sqrt{4\pi k_B T}} \exp\left[-(\Delta G^0 + \lambda)^2 / 4\lambda k_B T\right] \qquad (4)$$

and the rate takes its semiclassical Marcus theory expression[10]:

$$k_{if} = \frac{2\pi}{\hbar} \left|V_{if}\right|^2 \frac{1}{\sqrt{4\pi k_B T}} \exp\left[-(\Delta G^0 + \lambda)^2 / 4\lambda k_B T\right], \qquad (5)$$

where λ denotes the reorganization energy induced by the electron or energy transfer and ΔG^0 is the change in Gibbs free energy during the reaction. When the reorganization energy λ is cast into contributions of both classical modes for the surrounding medium [(λ_0); $\omega_h << k_B T$] and intramolecular high-frequency vibrational modes [(λ_i); $\omega_i >> k_B T$], the rate k_{if} becomes in the context of the Bixon and Jortner model (for details, see the review in Ref. 9):

$$k_{if} = \frac{2\pi}{\hbar} \left|V_{if}\right|^2 \sqrt{\frac{1}{4\pi\lambda_0 k_B T}} \sum_{n=0}^{\infty} \exp(-S_i) \frac{S_i^n}{n!} \times \exp\left(-\frac{(\Delta G^0 + \lambda_0 + n\hbar\omega_i)^2}{4\lambda_0 k_B T}\right). \qquad (6)$$

Here, a single effective quantum mode ω_i is assumed to contribute to λ_i. The Huang–Rhys factor, $S_i = \lambda_i / \omega_h$, is a measure of the electron-vibrational coupling interaction. The main effect of high-frequency modes is to renormalize the electronic coupling parameter rather than to contribute to the temperature dependence (except at high temperatures). This discussion underlines that, in order to achieve a complete understanding of the electron or energy transfer properties, a detailed knowledge of the vibrational modes coupled to the transfer process and of the electron-vibration constants is required.

3 Charge recombination in EL oligomers and polymers

From our discussion in the Introduction, it is clear that the efficiency of organic light-emitting diodes (LEDs) depends to a large extent on the nature of the excited species that are formed upon recombination of injected positive and negative charges. These excitations are known to be a function of both electron-vibration and electron-electron interactions; they are generally believed to be excitons with a binding energy in excess of kT.[11]

Of importance is that singlet and triplet excitons possess different energies; the singlet–triplet energy difference, that is the exchange energy, is estimated to be larger than 0.5 eV for the lowest excitation in a range of conjugated polymers.[12–16] They also display different geometry relaxations; due to the possibility of exchange between like spins, triplet wavefunctions usually display a more spatially confined character, a feature that is especially pronounced for low-lying excitations.[17] As we discuss below, the different nature of the singlet and triplet excitations has a profound impact on the theoretical upper limit for the quantum yields achievable in LEDs.

The quantum efficiency for electroluminescence (photoluminescence), η_{EL} [η_{PL}], is defined as the ratio between the number of photons coming out of the device and the number of electrons injected (photons absorbed). In π-conjugated oligomers and polymers, when triplets are not emissive, the ratio η_{EL}/η_{PL} is controlled by the fraction of singlet excitons generated in the diode (hereafter referred to as η_2). For a long time, this ratio was thought to follow simple spin multiplicity rules according to which η_{EL}/η_{PL} should not exceed 25% (since the recombination of an electron–hole pair – both spin $^1/_2$ – leads to a total of four microstates with three triplet states and one singlet state).

It must be clearly stated that this issue remains controversial[18] even if there now exists some compelling experimental[19–24] and theoretical[25–29] evidence that, *in conjugated polymers*, larger ratios between EL and PL quantum yields can be achieved. This stresses the possibility of producing highly efficient polymer LEDs and raises fundamental questions about the mechanisms determining exciton formation, which we now review.

Cao *et al.* found that upon improving the electron-transport properties of a substituted poly(*p*-phenylenevinylene)-based LED device, the ratio of external quantum efficiencies of EL with respect to PL can reach a value as high as 50%.[19] Values of η_2 ranging from 0.35 to 0.45 have also been reported by Ho *et al.* in PPV derivatives.[20a] Wohlgenannt *et al.* have measured η_2 by using a photo-induced absorption detected magnetic resonance (PADMR) technique for a large number of π-conjugated polymers and oligomers; the experimental η_2 values were found to increase with conjugation length ranging from ~0.25 in monomers to much larger values in extended π-conjugated systems.[21] Similarly, Wilson *et al.* have reported a singlet generation fraction close to 57% in a platinum-containing conjugated polymer, while a much smaller value (22%) was inferred for the corresponding monomer.[20b] The recent work at Philips is especially important in this regard and suggests quantum yields on the order of 60% in polymer LEDs based on poly(*p*-phenylenevinylene) or poly(spirobifluorenes).[24] From these experimental data, the emerging picture is that η_2 follows closely spin statistics in small conjugated oligomers or molecules[30] while the 25% statistical limit can be significantly overcome in polymers.

Charge recombination between an injected electron and an injected hole appears to occur as a two-step process.[23] In the first step, the initially fully separated charges coalesce into loosely bound singlet or triplet polaron pairs, also referred to as charge-transfer (CT) excitons. In a second step, these intermediate states then decay into lower singlet or triplet neutral exciton states. Two major aspects need to be emphasized:

(i) Since the first step can only obey spin statistics, when the second step is faster than any other process affecting the intermediate CT states, *spin statistics is followed*. Thus, overcoming spin statistics requires that the second step be significantly slower for triplet than for singlet CT states. Then, either of two things can happen. Intersystem crossing can switch triplet pairs into singlet pairs[31,32] that could decay down the singlet exciton manifold; or triplet pairs can have time to dissociate and some of the freed charges can later reassociate as singlet pairs.

(ii) Baessler and co-workers[33] have recently shown, *via* thermoluminescence measurements on phenylene-based materials, that the singlet–triplet splitting among the CT states (polaron pairs) is merely on the order on 3–6 meV (depending on polymer morphology); thus, the possibility exists for intersystem crossing or possibly dissociation of the CT states.

If we denote by σ_S and σ_T the cross-sections for formation of neutral singlet and triplet exciton states, the expression for η_2 can be written as

$$\eta_2 = \sigma_S/(\sigma_S + 3\sigma_r) = \sigma_{S/T}/(\sigma_{S/T} + 3), \qquad (7)$$

where $\sigma_{S/T} = \sigma_S/\sigma_T$. For $\sigma_S = \sigma_T$. For $\sigma_S = \sigma_T$, we get $\eta_2 = 25\%$, the statistical limit; η_2 becomes 50% for $\sigma_S = 3\sigma_T$; for $\sigma_T = 0$, $\eta_2 = 100\%$.

Bittner and co-workers have developed a methodology based on the particle-hole picture of solid-state physics that allows the simulation of the dissipative dynamics of an extended one-dimensional polymer system coupled to a phonon bath.[26,27] When applying this formalism to a quantum molecular dynamics simulation of the formation of exciton states from polaron pairs, they found a clear correlation between the rates for *intrachain* generation of singlet-and-triplet excitons on a single long PPV segment and the corresponding binding energy: the ratio σ_S/σ_T was calculated to evolve linearly with the singlet to triplet binding energy ratio.[27] This evolution was explained in terms of spin specific energetics and mutual vibronic couplings between the excited states on an isolated polymer chain. Below, it is argued that the rate limiting step is the *interchain* charge recombination process from the CT states into the manifold of intrachain singlet-and-triplet excitons (followed by faster downhill internal conversion driven by vibronic couplings). Mazumdar and co-workers also reported chain-length-dependent formation cross sections for *interchain* charge recombination, based on exact calculations for small polyene chains.[28]

We now discuss the results of calculations aimed at exploring the *chain-length dependence* of the singlet- and triplet-formation cross sections in conjugated materials.[34] It is important to stress that both the electronic couplings and energetics of the charge recombination process were accounted for in this work by applying a standard Jortner formulation for the calculation of charge recombination rates.[9] Different generation rates are obtained for the singlet and triplet excitons due to the different nature of these excited states, which impacts their relative energies and gives rise to different electronic tunnelling matrix elements for charge recombination. Most importantly, *the formation rates of singlet over triplet neutral excitons is found to vary significantly with chain length*.

3.1 Theoretical aspects

The σ_S and σ_T cross sections can be calculated in the framework of perturbation theory and the Fermi Golden Rule, as described in the Introduction. In order to compute the electronic coupling V_{if}, the singlet and triplet-excited state wave functions were obtained for unrelaxed geometries by combining a Pariser–Parr–Pople (PPP) Hamiltonian to a single configuration interaction (SCI) scheme. The lowest-lying charge transfer state is taken as the initial state in the recombination process; this state is described by a single determinant built by promoting an electron from the HOMO of one chain to the LUMO of an adjacent chain. This is reasonable since the electron (hole) can relax from higher unoccupied (lower occupied) orbitals to the lowest (highest) one, prior to recombination. To account for the polarization effects induced by the medium, the energies of the excitonic and polaronic species were computed at the AM1(CI) level within the continuum dielectric approximation through the use of a COSMO approach.[35] We also considered the Coulomb stabilization E_{cb} of the initial state in the recombination process, which in the model corresponds to a pair of opposite charges lying on adjacent conjugated segments; this stabilization can be estimated on the basis of the charge density distributions in the positive and negative polarons:

$$E_{cb} = \sum_i \sum_j \frac{q_i}{\varepsilon_s} \frac{q_j}{r_{ij}}, \qquad (8)$$

where q_i (q_j) is the charge on site i (j) in the positively (negatively) charged molecule, as calculated with a Mulliken population analysis at the AM1/CI-COSMO level, and r_{ij} the distance between sites i and j; ε_s is the medium static dielectric constant, which is taken both in Eq. (8) and the COSMO calculations to be equal to 4, a typical value for the dielectric constant of organic conjugated polymers.[36,37] The energy separation between the initial charge separated state and the lowest excited state for the singlet process then can be written as:

$$\Delta_S = E(P^+) + E(P^-) - 2\times E(S_0) - E(S_1) + E_{cb}, \qquad (9)$$

where $E(P^+)$, $E(P^-)$, $E(S_0)$, and $E(S_1)$ correspond to the energies in their relaxed geometries of the positive and negative polarons and the singlet ground and excited states, respectively. Note that Δ_S is the driving force, ΔG^0, for the charge recombination reaction into S_1; the changes in Gibbs free-energy relative to the processes yielding higher-lying

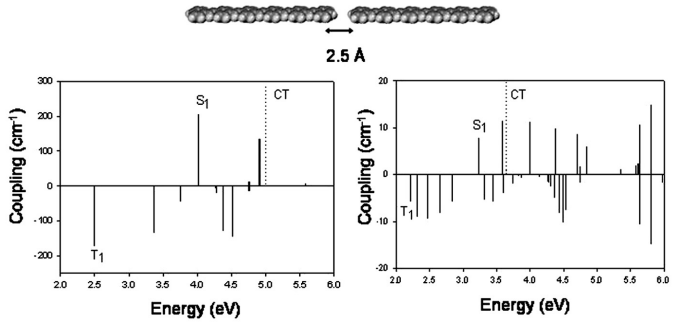

FIGURE 2 — Top: Illustration of the head-to-head configuration between two OPV6 oligomers. Bottom: Charge recombination electronic couplings, V_{if}, into singlet and triplet excited states in head-to-tail dimers of OPV2 (left) and OPV6 (right) molecules. Note the change in scale for the couplings (by a factor of 15) between OPV2 and OPV6. The molecular packing is shown on top.

singlet S_n states or triplet T_n excited states are obtained by adding to Δ_S the $S_n - S_1$ or $T_n - S_1$ energy difference as provided by the PPP/SCI scheme (for such processes, the entropy effects can be neglected).

We considered a two-chain model with two possible orientations for the conjugated chains, see top of Figs. 1 and 2. While "interchain" electron or hole hopping between adjacent chains lying in a cofacial (or, more generally H-type) arrangement is the most likely scenario in short chains, migration of the charges between conjugated segments on the same chain is also possible in longer (polymer) chains; the head-to-tail configuration in Fig. 2 is intended to model such an "intrachain" process. The calculations were performed on phenyl-capped phenylene vinylene oligomers ranging in size from 2 to 10 phenylene rings; hereafter, we only refer to the results obtained for oligomers containing two rings, OPV2 (the trans-stilbene molecule) and six rings, OPV6; these are taken as representatives for "small molecules" and "polymer chains," respectively.

3.2 Chain-length dependence of singlet and triplet exciton formation rates

The spin-dependent recombination process from charge-transfer states to neutral exciton states (the second step described above) can be depicted as an electron-transfer reaction. Thus, in the context of Eq. (6), we will discuss consecutively the impact of (i) the electronic couplings (matrix elements), V_{if}; (ii) the driving force, ΔG^0; and (iii) the inner and outer reorganization energies, λ.

Electronic couplings: The main results are collected in Figs. 1 and 2, which show the electronic couplings between the CT states and the singlet and triplet excitons as a function of excitation energy, and in Fig. 3, which displays the evolution with chain length of the ratio between the electronic couplings into S_1 and T_1.

In the cofacial arrangements, the largest matrix elements are calculated for the lowest singlet S_1 and triplet T_1 excited states, in agreement with previous works.[25,28] This feature can be readily explained on the basis of the overlap

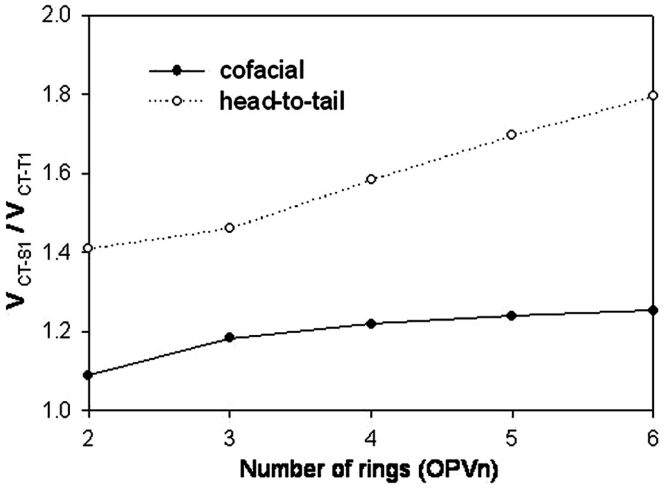

FIGURE 3 — Evolution with chain length of the ratio between the exciton formation electronic couplings, V_{if}, into the lowest singlet and triplet excited states, in cofacial (solid line) and head-to-tail (dashed line) configurations.

between the wavefunctions of the initial and final states. Since the initial charge-transfer state is assumed to be a pure transition from the HOMO of one chain to the LUMO of the other chain, optimal overlap is achieved with the final excited state that involves the largest contributions from these frontier orbitals, *i.e.*, the lowest-lying singlet and triplet states. Note that the system in the cofacial arrangement possesses C_{2h} symmetry; only B_u-symmetry excited states are then allowed to couple electronically to the B_u-symmetry CT state.

The situation is somewhat different for the head-to-tail configurations, where a number of different singlet and triplet excited states show significant electronic couplings to the charge-transfer state; this is partly due to the reduced symmetry of the head-to-tail arrangement. Here, chain-end contributions to the wavefunctions play a major role. A clear correlation can be found between the magnitude of the interchain matrix elements and the shape of the excited-state wavefunctions, with more delocalized excited states leading to larger couplings.

While in head-to-tail aggregates, the ratio between the matrix elements for charge recombination to yield S_1 *vs.* T_1 is hardly chain-length dependent, the corresponding ratio shows a marked increase in the case of cofacial arrangements. This comes from the different nature of the lowest singlet and triplet excited states, the latter being more localized around the central part of the chain.[17] As expected, the differences in the spatial confinements of the S_1 and T_1 wavefunctions are amplified in the head-to-tail configurations for which contributions at the edges of the conjugated segments are the most relevant.

It is useful to recall that electronic excitations in phenylene-based materials can be classified into three categories, depending on the nature of the involved molecular orbitals (MOs)[38,39]:

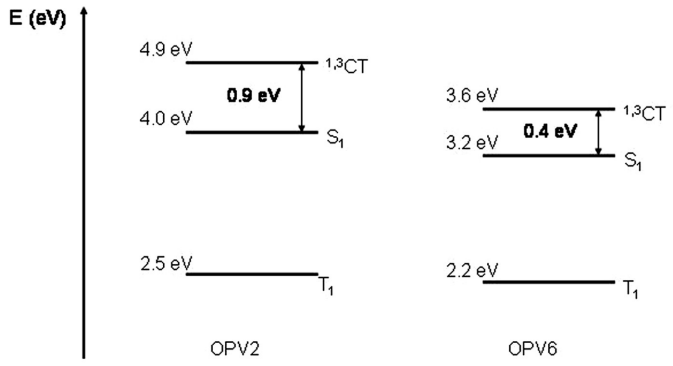

FIGURE 4 — Schematic energy diagram showing the position of the lowest on-chain singlet, S_1, and triplet, T_1, excited states and the lowest charge-separated states, ^{1}CT and ^{3}CT, in a cofacial stack made of two OPV2 and OPV6 oligomers.

*dd** excitations, built by promoting an electron from an occupied delocalized MO to an empty delocalized MO;

*ll** excitations, involving only orbitals that are localized on the phenylene rings; and

dl/ld** excitations, which correspond to transitions from occupied delocalized orbitals to unoccupied localized orbitals and vice-versa.

Figure 1 indicates that in cofacial aggregates there is a series of excited states, lying about 4.0–5.0 eV above the ground state, with recombination matrix elements on the order 10–30 cm^{-1}; in this spectral range, singlet and triplet excited states show similar electronic couplings, though slightly larger for the triplets. These high-lying excited states are assigned mainly to mixed *dl*/ld** and, to a lesser extent, *ll**-type excitations. Because of their reduced electron-hole overlap, the singlet and triplet *dl*/ld** excited states are almost degenerate, display similar wavefunctions, and hence lead to nearly equal charge recombination cross sections. As described below, these states could play an important role in the exciton formation mechanism in small molecules. In head-to-tail configurations, Fig. 2, the situation is more complex; higher-lying *dd** excitations acquire significant coupling with the charge-transfer state as a result of the lower symmetry of the dimers and close contacts between the edges of the conjugated segments. It should be noted that the magnitude of the electronic couplings drops much more quickly with chain length in head-to-tail *vs.* cofacial dimers, a feature that has also been underlined in the case of excitonic energy-transfer processes.[40]

Driving force: Figure 4 provides a schematic energy diagram with the relevant electronic states for the OPV2 and OPV6 model systems (assuming a distance between the molecular planes of 4 Å in a cofacial dimer). For both chains, the lowest intrachain singlet excited state lies *below* the charge separated state, which is consistent with the view that primary photoexcitations in PPV are on-chain excitations and not polaron pairs.[41,42] The most important result is that the energy gap Δ_S between S_1 and ^{1}CT decreases significantly when going from OPV2 ($\Delta_S \sim 0.9$ eV) to OPV6 ($\Delta_S \sim 0.4$ eV).

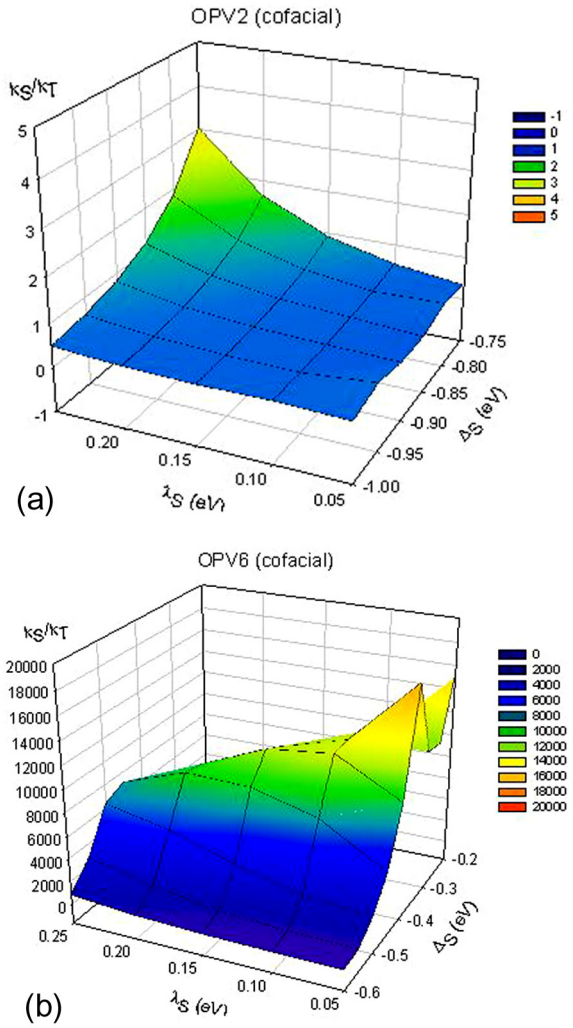

FIGURE 5 — Ratio between the singlet and triplet charge recombination rates, $r = k_S/k_T$, as a function of Δ_S and λ_S, in a cofacial arrangement of two (a) OPV2 and (b) OPV6 chains.

Reorganization energy: The inner part, λ_i, corresponds to the energy required to switch from the geometry of two oppositely charged polarons (forming the charge transfer state) to the equilibrium geometry of the target excited state on one chain and the ground-state geometry on the other chain. Due to the close similitude of the geometric distortions induced by charge injection or neutral excitation in a conjugated chain (at least for the lowest singlet excited state),[43] we expect this contribution to be on the order of the polaron relaxation energy. We have therefore chosen a λ_i value of 0.15 eV, which together with an effective frequency mode of 0.15 eV leads to a Huang–Rhys factor S = 1. Because of the low dielectric constant of organics and the short separation between the positive and negative charges in the charge-transfer state, the solvent contribution to the relaxation energy ought also to be small, on the order of that found in weakly polar solvents, typically a few tenths of an eV.

The different approximations that we were forced to take do not allow quantitative predictions of the exciton formation rates. However, we have made sure that the choice

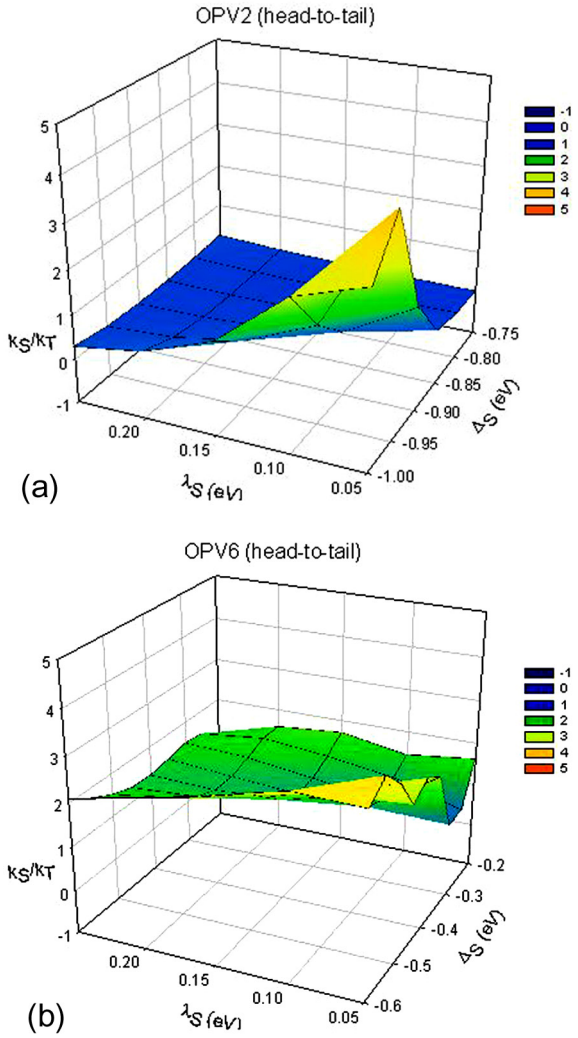

FIGURE 6 — Ratio between the singlet and triplet charge recombination rates, $r = k_S/k_T$, as a function of Δ_S and λ_S, in a head-to-tail arrangement of two (a) OPV2 and (b) OPV6 chains.

of molecular parameters used in the simulations does not affect the overall picture, by applying Eq. (6) to a range of λ_s and Δ_S values. The resulting ratios between singlet and triplet exciton generation rates, $r = k_S/k_T$ (where k corresponds to the sum over all pathways in a given manifold), are reported as two-dimensional grids in Figs. 5 and 6. As expected, the absolute values of the rates are very sensitive to the relative magnitude of the driving force with respect to the reorganization energy, which according to a classical view fixes the height of the barrier for the recombination reaction. However, the important results are the following:

(i) For most of the $\{\lambda_s, \Delta_S\}$ space explored, the k_S/k_T ratio is *smaller or close to one in OPV2 while it is much higher in OPV6* (especially in the cofacial configuration).

(ii) In spite of the relatively small electronic couplings, the calculated recombination rates at room temperature are relatively fast (they somewhat vary as a function of the actual values chosen for the reorganization energy and driving force): in OPV2, on the order of 10^9–10^{10} sec^{-1} for *both* singlets and triplets; in OPV6, ca. 10^{10}–10^{11} sec^{-1} for singlets but *significantly smaller*, 10^7–10^8 sec^{-1}, *for triplets*.

These results can be understood in the following way. For small molecules in a face-to-face arrangement, the rather large energy separation between the charge-transfer state and the lowest singlet excited state reduces the efficiency of the direct S_1 generation. In this case, higher-lying singlet S_n states, closer in energy and electronically coupled to the initial charge transfer state, are formed with a higher probability; these include the *dl*/ld** excitations. Since these excited states are only weakly split by exchange interactions, the corresponding triplet T_n excited states have comparable excitation energies, wavefunctions, electronic couplings, and therefore recombination rates. It follows that, in short oligomers, singlets and triplets form with comparable probabilities and spin statistics is pretty much obeyed. In contrast, the S_1 pathway is dominant in long chains due to the reduced $S_1 - {}^1CT$ energy gap and the larger tunnelling matrix element associated to that state. Since S_1 shows the largest electronic coupling, the singlet route is favored over the triplet channel in extended systems; *this results in ratios between singlet and triplet formation rates largely exceeding one.* The situation is more complex in head-to-tail arrangements where higher-lying *dd** excited states also play a significant role. In all cases, direct formation of T_1 is very unlikely due to the very large change in Gibbs free energy (on the order of 1.5 eV in OPV6 and larger than 2 eV in OPV2), which sets this process into the inverted Marcus region.[44]

While the mechanism proposed above specifically applies to phenylene-based materials (for which different types of excitations are encountered), the results can be generalized to a number of other conjugated polymers. Indeed, in the simplest one-dimensional two-band model (such as the one used to describe the excited states in polyenes),[45] the average electron-hole separation of the on-chain excitations goes up with increasing energy. Hence, high-lying excited states are less subject to exchange interactions, which decay exponentially with distance. Since it can be reasonably expected that only these higher-energy states are reached efficiently in small molecules or oligomers, this will result in singlet and triplet formation rates of comparable magnitudes. In extended π-systems, contributions from the lowest excited state should dominate the mechanism of singlet generation, because of both large electronic recombination matrix elements and small energy barriers. This process is expected to occur at a faster rate than the formation of any triplet T_n excited state; hence, neutral triplet excitons should be created at a lower rate than singlets, opening the way to deviations from spin statistics.

Using transient spectroscopic techniques, Wohlgenannt *et al.* have measured the formation cross-section ratio of singlet and triplet excitons in a variety of π-conjugated materials.[46] They found a universal relationship

between the low-energy polaron absorption and the chain length in oligomers and, on that basis, showed that the larger the conjugation length, the higher the singlet population. Their experimental data also indicate that the formation cross-section ratio increases in the following sequence: 6T [sexithiophene] < PPE [poly(*p*-phenyleneethynylene)] < PPV < RRaP3HT [regio-random poly(hexylthiophene)] < mLPPP [ladder-type poly(*p*-phenylene)] < RR-P3HT [regio-regular poly(hexylthiophene)]. This trend might be due to material-dependent Δ_S values (*i.e.*, the energy separation between S_1 and the lowest charge transfer or polaron pair state), rather than changes in the singlet exciton binding energy (*i.e.*, the energy difference between S_1 and the single particle continuum). Δ_S is very sensitive not only to the chemical structure of the individual conjugated chains but also to the way the chains pack in the solid state, with the lowest values found in the most highly ordered materials. The largest ratios between singlet and triplet yields measured for RR-P3HT and mLPPP suggest that small Δ_S values (these two materials display a high degree of both intrachain and interchain order) translate into efficient singlet generation.

4 Synopsis

We have reviewed the mechanisms of singlet and triplet exciton formation in electroluminescent π-conjugated materials. The main conclusions can be drawn as follows:

(i) Deviations from simple spin statistics (according to which only one-fourth of the excitons are formed as singlets) can occur if triplet charge-transfer excited states (polaron pairs) are amenable to intersystem crossing or dissociation.

(ii) The electronic couplings between the charge-transfer states and the neutral exciton states are predicted to be largest for S_1 and T_1. However, because of the large exchange energy K ($S_1 - T_1$ energy difference), the probability for direct recombination into T_1 is, in all cases, very small (Marcus inverted regime).

(iii) In small molecules, the CT – S_1 energy difference is large. Both singlet and triplet exciton formations proceed *via* higher-lying S_n/T_n states, which display similar electronic couplings and are therefore characterized by similar formation rates. These rates are fast and, as a result, spin statistics is expected to be obeyed.

(iv) In extended conjugated chains, the energy difference between the CT and S_1 excited states becomes on the order of the reorganization energy, *i.e.*, a few tenths of an eV; in a Marcus picture, *this leads to the smallest barriers*. As a result, the ^{1}CT → S_1 pathway tends to be even faster than in small molecules. On the contrary, the ^{3}CT → T_n channels become much slower, leaving room for intersystem crossing or dissociation among the ^{3}CT states.

In a simplified picture, these results suggest that making smaller the energy separation between the charge transfer state and the lowest singlet exciton state, can increase the relative generation of singlets versus triplets. It would follow that highly ordered materials (with short intermolecular contacts and delocalized charges) should have the largest singlet/triplet ratios. However, this does not necessarily imply that the highest quantum yields could be reached. Indeed, by reducing the energy separation between intrachain and interchain excitations, the relative population of non-emissive polaron pair species should also increase, which could potentially impact the balance between radiative and non-radiative decay channels. Thus, there is a need to develop materials where an optimal compromise can be achieved between singlet exciton generation and luminescence efficiency.

Acknowledgments

The work on light-emitting π-conjugated materials at Georgia Tech has been partly supported by the National Science Foundation (through the STC Program under Award Number DMR-0120967 and grant CHE-0342321), the Office of Naval Research, the Georgia Tech "Center on Organic Photonics and Electronics (COPE)," and the IBM Shared University Research Program; the work in Mons, by the Belgian Federal Government "InterUniversity Attraction Pole in Supramolecular Chemistry and Catalysis (PAI 5/3)," the European Commission project STEPLED (IST-2001-3735), and the Belgian National Fund for Scientific Research (FNRS). DB is an FNRS Research Fellow; and the work in Beijing, by the National Science Foundation of China (Grant No. 90203015) and the Ministry of Science and Technology of China (973 programme Grant No. 2002CB613406).

References

1 C K Chiang, Y W Park, A J Heeger, H Shirakawa, E J Louis, and A G MacDiarmid, *Phys Rev Lett* **39**, 1098 (1997).

2 See, for instance, *Handbook of Conducting Polymers, 2nd Edition*, Eds, T. A. Skotheim, J. R. Reynolds, and R. L. Elsenbaumer (Marcel Dekker, New York, 1997).

3 C W Tang and S A VanSlyke, *Appl Phys Lett* **51**, 913 (1987).

4 J H Burroughes, D D C Bradley, A R Brown, R N Marks, R H Friend, P L Burn, and A B Holmes, *Nature* **347**, 539 (1990).

5 R H Friend, R W Gymer, A B Holmes, J H Burroughes, R N Marks, C Taliani, D D C Bradley, D A dos Santos, J L Brédas, M Lögdlund, and W R Salaneck, *Nature* **397**, 121 (1999).

6 J R Sheats, H Antoniadis, M Hueschen, W Leonard, J Miller, R Moon, D Roitman, and A Stocking, *Science* **273**, 884 (1996).

7 H Sirringhaus, T Kawase, and R H Friend, *Science* **290**, 2123 (2000).

8 *Electron Transfer in Chemistry,* Ed., Balzani V. (Wiley-VCH, Weinheim, 2001).

9 "Electron Transfer: From Isolated Molecules to Biomolecules," *Adv Chem Phys* **106–107** (Eds., Bixon, M. and Jortner, J.) (Wiley, New York, 1999).

10 R A Marcus, *Reviews of Modern Physics* **65**, 599 (1993); *J Chem Phys* **24**, 966, 979 (1956); R A Marcus and N Sutin, *Biochimica Biophysica Acta* **811**, 265 (1985).

11 *Primary Photoexcitations in Conjugated Polymers: Molecular Exciton versus Semiconductor Band Model,* Ed., Sariciftci, N. S. (World Scientific, Singapore, 1997).

12 N Chawdhury, A Köhler, R H Friend, W-Y Wong, J Lewis, M Younus, P R Raithby, T C Corcoran, M R A Al-Mandhary, and M S Kahn, *J Chem Phys* **110**, 4963 (1999).
13 A Köhler, J S Wilson, R H Friend, M K Al-Suti, M S Khan, A Gerhard, and H Bässler, *J Chem Phys* **116**, 9457 (2002).
14 A P Monkman, H D Burrows, L J Hartwell, L E Horsburgh, I Hamblett, and S Navaratnam, *Phys Rev Lett* **86**, 1358 (2001).
15 Y V Romanvskii, A Gerhard, B Schweitzer, U Scherf, R I Personov, and H Bässler, *Phys Rev Lett* **84**, 1027 (2000).
16 D Hertel, S Setayesh, H G Nothofer, U Scherf, R I Personov, and H Bässler, *Adv Mater* **13**, 65 (2001).
17 D Beljonne, Z Shuai, R H Friend, and J L Brédas, *J Chem Phys* **102**, 2042 (1995).
18 M Segal, M A Baldo, R J Holmes, S R Forrest, and Z G Soos, *Phys Rev B* **68**, 075211 (2003).
19 Y Cao, I D Parker, G Yu, C Zhang, and A J Heeger, *Nature* **397**, 414 (1999).
20 P K H Ho, J Kim, J H Burroughes, H Becker, S F Y Li, T M Brown, F Cacialli, and R H Friend, *Nature* **404**, 481 (2000); J S Wilson, A S Dhoot, A J A B Seeley, M S Khan, A Köhler, and R H Friend, *Nature* **413**, 828 (2001).
21 M Wohlgenannt, K Tandon, S Mazumdar, S Ramasesha, and Z V Vardeny, *Nature* **409**, 494 (2001); M Wohlgenannt, X M Jiang, Z V Vardeny, and R A J Janssen, *Phys Rev Lett* **88**, 197401 (2002).
22 A S Dhoot, D S Ginger, D Beljonne, Z Shuai, and N C Greenham, *Chem Phys Lett* **360**, 195 (2002).
23 T Virgili, G Cerullo, L Lüer, G Lanzani, C Gadermaier, and D D C Bradley, *Phys Rev Lett* **90**, 247402 (2003).
24 E A Meulenkamp, R van Aar, J J A M Bastiaansen, A J M van den Biggelaar, H Börner, K Brunner, M Büchel, A van Dijken, N M M Kiggen, M Kilitziraki, M M de Kok, B M W Langeveld, M P H Ligter, S I E Vulto, P van de Weijer, and S H P M de Winter; *SPIE - The International Society for Optical Engineering* (in press).
25 Z Shuai, D Beljonne, R J Silbey, and J L Brédas, *Phys Rev Lett* **84**, 131 (2000).
26 M N Kobrak and E R Bittner, *Phys Rev B* **62**, 11473 (2000).
27 S Karabunarliev and E R Bittner, *Phys Rev Lett* **90**, 057402 (2003).
28 K Tandon, S Ramasesha, and S Mazumdar, *Phys Rev B* **67**, 045109 (2003).
29 T Hong and H Meng, *Phys Rev B* **63**, 075206 (2003).
30 M A Baldo, D F O'Brien, M E Thompson, and S R Forrest, *Phys Rev B* **60**, 14422 (1999).
31 E L Frankevich, A A Lymarev, I Sokolik, F E Karasz, S Blumstengel, R H Baughman, and H H Hörhold, *Phys Rev B* **46**, 9329 (1992).
32 V Dyakonov, G Rösler, M Schwoerer, and E L Frankevich, *Phys Rev B* **56**, 3852 (1997).
33 A Kadashchuk, A Vakhnin, I Blonski, D Beljonne, Z Shuai, J L Brédas, V I Arkhipov, P Heremans, E V Emelianova, and H Bässler, *Phys Rev Lett* **93**, 066803 (2004).
34 D Beljonne, A Ye, Z Shuai, and J L Brédas, *Adv Funct Mat* **14**, 684 (2004).
35 A Klamt and G Schürmann, *J Chem Soc Perkin Trans* **2**, 799 (1993); J Tomasi and M Persico, *Chem Rev* **94**, 2027 (1994).
36 D Comoretto, G Dellepiane, F Marabelli, J Cornil, D A dos Santos, J L Brédas, and D Moses, *Phys Rev B* **62**, 10173 (2000).
37 J W van der Horst, P A Bobbert, P H L de Jong, M A J Michels, G Brocks, and P J Kelly, *Phys Rev B* **61**, 15817 (2000). According to these authors, it is the perpendicular dielectric constant that plays the dominant role in the interchain screening along the chain; a value of ~3 was calculated for that component.
38 J Cornil, D Beljonne, R H Friend, and J L Brédas, *Chem Phys Lett* **223**, 82 (1994).
39 M Chandross, S Mazumdar, M Liess, P A Lane, Z V Vardeny, M Hamaguchi, and K Yoshino, *Phys Rev B* **55**, 1486 (1997).
40 D Beljonne, G Pourtois, C Silva, E Hennebicq, L M Herz, R H Friend, G D Scholes, S Setayesh, K Müllen, and J L Brédas, *Proc Natl Acad Sci USA* **99**, 10982 (2002); E Hennebicq, G D Pourtois, Scholes, L M Herz, D M Russell, C Silva, S Setayesh, K Müllen, J L Brédas, and D Beljonne, *J Am Chem Soc* (in press).
41 G R Hayes, I D W Samuel, and R T Philipps, *Phys Rev B* **52**, 11569 (1995).
42 N T Harrison, G R Hayes, R T Philipps, and R H Friend, *Phys Rev Lett* **77**, 1881 (1996).
43 J L Brédas, J Cornil, and A J Heeger, *Adv Mater* **8**, 447 (1996).
44 R A Marcus, *J Chem Phys* **43**, 679 (1965).
45 D Guo, S Mazumdar, S N Dixit, F Kajzar, F Jarka, Y Kawabe, and N Peyghambarian, *Phys Rev B* **48**, 1433 (1993).

David Beljonne received his Ph.D. in chemistry from the University of Mons-Hainaut in 1994. After a postdoctoral stay at the University of Cambridge (with Prof. Sir Richard Friend) and the University of Rochester (with Prof. Shaul Mukamel), he is presently a Senior Research Associate of the Belgian National Science Foundation in Mons and a Visiting Principal Research Scientist at Georgia Tech. His work deals with a theoretical characterization of the nature and dynamics of electronic excitations in conjugated polymers and molecules.

Zhigang Shuai received his Ph.D. in physics from Fudan University in Shanghai, PR China, in 1989. He then moved to Jean-Luc Brédas' group at the University of Mons-Hainaut, Belgium, first as a postdoc, then as a senior research scientist, for about 12 years. In 2002, he was appointed as a Full Professor in the Key Laboratory of Organic Solids, Institute of Chemistry of the Chinese Academy of Sciences (ICCAS) in Beijing, where is currently Head of Theory of Organic Solids. Since 2002, he is in charge, as one of the two Chair Scientists, of the "Organic and Polymeric Light-Emitting Materials" program, a key basic research plan from the Ministry of Science and Technology of China. He has been awarded a "Hundred Talents Plan" from the Chinese Academy of Sciences and he is the recipient of the prestigious "Outstanding Young Scientist Award" from the National Science Foundation of China. His main interests are in the theoretical physics and theoretical chemistry of organic and polymeric materials and devices.

Aijun Ye received his Ph.D. in chemistry from the University of Mons-Hainaut in 2002. After postdoctoral research at the University of Mons-Hainaut and the University of Houston, he is presently a postdoctoral fellow at the Georgia Institute of Technology with Jean-Luc Brédas. His work deals with the theoretical investigation of the optical and electronic properties of conjugated polymers and molecules.

Jean-Luc Brédas received his Ph.D. in chemistry from the University of Namur, Belgium, in 1979. After a joint postdoctoral stay at MIT and the (then) Allied Chemical Corporate Research Center in Morristown, New Jersey, he went back to Namur in 1981 as a Research Fellow of the Belgian National Science Foundation. In 1988, he was appointed Professor at the University of Mons-Hainaut, Belgium, and Head of the Laboratory for Chemistry of Novel Materials. While keeping an "Extraordinary Professorship" appointment in Mons, Jean-Luc Brédas joined the University of Arizona in 1999 before moving in 2003 to the Georgia Institute of Technology where he is Professor of Chemistry and Biochemistry. He is the recipient of the 1997 Francqui Prize, the 2000 Quinquennial Prize of the Belgian National Science Foundation, the 2001 Italgas Prize for Research and Technological Innovation (shared with Richard Friend), and a member of the team laureate of the 2003 Descartes Prize of the European Union. Since 2001, he is a member of the European Research Advisory Board (EURAB) for Science, Technology, and Innovation. The research interests of his groups focus on the computational design of novel organic materials with remarkable electrical and optical properties.